The Monte Carlo Method: Versatility Unbounded In A Dynamic Computing World
Chattanooga, Tennessee, April 17–21, 2005, on CD-ROM, American Nuclear Society, LaGrange Park, IL (2005)

Consequences of Regular and Irregular Beam Impact on the LHC Collimators

Vlachoudis V*, Assmann R, Ferrari A, Magistris M,
Santana-Leitner M, Tsoulou E
CERN
CH-1211 Geneva-23
Switzerland
Corresponding Address: Vasilis.Vlachoudis@cern.ch

ABSTRACT

The Large Hadron Collider (LHC) collimators must be able to withstand at 7 TeV/c the shock impact of about 8 out of the 2808 circulating bunches, as well as continuous beam losses for reduced beam lifetimes. These are strict requirements, given the 350 MJ of stored beam energy in the LHC and the small spot size at 7 TeV/c. The consequences of beam impact on the collimators were calculated for various scenarios and then used as input to FLUKA showering studies. Detailed loss maps and shower calculations are employed to predict maximum equipment heating in the LHC cleaning insertions and the subsequent requirements for equipment design, cooling, and additional absorbers.

Key Words: LHC, Collimation, FLUKA, Simulation

1 INTRODUCTION

The LHC will produce proton-proton collisions at a center-of-mass energy of 14 TeV with unprecedented high beam intensities. For nominal performance it is planned to fill 2808 bunches of 1.1×10^{11} protons each. Both LHC beams will store 3×10^{14}, 7 TeV protons, resulting in beam energy of 350 MJ. This high beam power must be handled in a super-conducting environment, severely constraining the fraction of the beam that can be lost in a super-conducting magnet. Even a tiny fraction of order of $1/10^9$ of the total beam power is sufficient to quench a magnet if it is deposited in its cold parts [1]. The LHC collimators are designed to restrict the mechanical aperture in the machine and to clean the primary halo so that quenches of magnets are avoided. Due to the high beam power LHC will be the first machine requiring the collimators to define the mechanical aperture through the whole cycle of the machine. Therefore the collimators must fulfill two purposes:

- Absorption of the beam halo which is created by regular processes such that only a small fraction of particles can impact in the cold aperture. The required suppression is of the order of 10^{-4} and collimators must sit at around 6 σ.
- Passive protection of the cold aperture in case of failures, both by absorbing part of the beam and by triggering beam abort for irregular losses.

The present paper describes in brief the challenging simulation work performed with the FLUKA [2,3] Intra-Nuclear cascade code. In the first part, the shower calculations in the

* Corresponding Author: Vasilis.Vlachoudis@cern.ch

collimators will be presented together with various beam failure cases that lead to the material choice for the jaws. The second part describes the simulations of the impact of the beam lost in the collimators on the super-conducting elements located in the dispersion suppressors next to the betatron cleaning area, along with the effect on a vital and costly part of the hardware, the controlling electronics.

2 COLLIMATORS MATERIAL CHOICE

The choice of materials for the LHC collimator jaws is not so much driven by the standard collimation procedures during the coast but rather by malfunctions of the components. The most significant "accident" scenarios are [4,5]:

- Faulty kick by the injection kicker where a full batch of protons hit the front of a collimator jaw at 450 GeV/c;
- Due to a spontaneous rise of one of the extraction kicker modules during the coast, part of the 7TeV/c beam is spread across the front of a collimator jaw.

It is well established that to intercept fast (several micro-seconds) bursts of multi-hundred GeV-beams, low Z-materials must be used [6]. Among other factors, this is due to the strong decrease of the radiation length with rising atomic charge (Z), which leads to a larger contribution of the electron-gamma part within the cascade and also to its more intense spatial concentration and thus to higher energy densities. Therefore the material studies have concentrated on Beryllium and Graphite while, for completeness, computations have also been made for heavier materials.

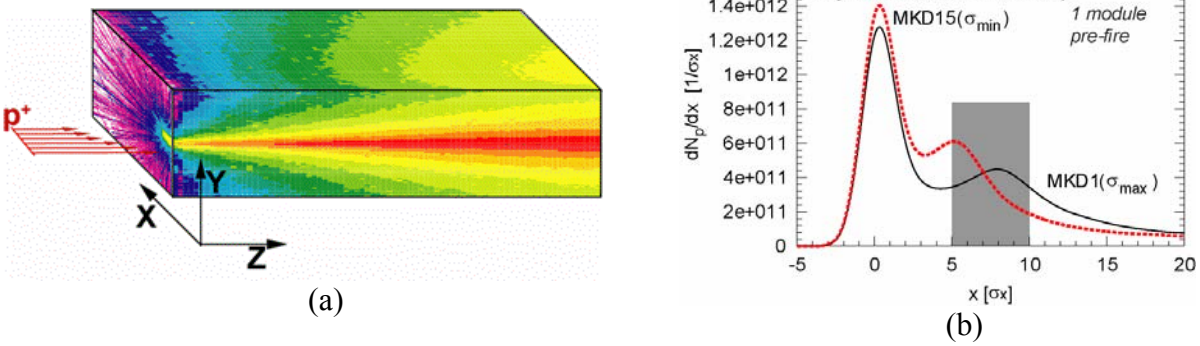

(a) (b)

Figure 1: (a) Simulated geometry of a single collimator jaw; (b) beam profile impacting the horizontal face of the collimator jaw.

FLUKA [2,3] simulates the proton interaction and the resulting cascade in a material from which the spatial energy densities are extracted. The simulation setup was rather simple, using a single jaw, with a rectangular shape with and/or without coating with dimensions $10\times5\times160$ cm^3 (Fig. **1**a). 8 bunches of 1.05×10^{11} p each of the 7 TeV/c proton beam are swept horizontally over about 1 mm across the front face of the collimator with a time-projected horizontal proton distribution given from the scenario of the dump failure of the single module pre-fire (Fig. **1**b). The impact parameter was varying in a range between $5\sigma - 10\sigma$ on the horizontal plane a Gaussian distribution on the vertical plane of $\sigma_x=\sigma_y=200$ μm. At these energies when the proton beam is grazing the surface of an object the multiple Coulomb scattering algorithm used in codes like FLUKA, can generate artifacts, resulting due to non-physical trajectories. Therefore this

algorithm was disabled for distances very close to the surface. The energy deposition was scored in a 3 dimensional grid, which was later converted to instantaneous temperature rise under adiabatic conditions.

In Table **I** the peak energy densities and the resulting instantaneous temperature rises are given for various materials, when hit by a 7 TeV beam. It clearly demonstrates that only Beryllium and Graphite may be considered. As mentioned above, these materials confine only a small part of the cascade, while the rest escapes from the collimator. This effect is further illustrated in Fig. **2**a, where the maximum energy densities are plotted versus its mass-length, to remove the pure effect of the density and hence revealing the strong Z-dependence. It shows that for all considered materials their respective peaks are reached at a depth of about 200 g/cm^2 while their values grow over-proportionally with the density. The instantaneous temperature rises in Graphite and Beryllium versus length are given in Fig. **2**b. Peak values of 800°C and 310°C are reached at Z=120 cm, respectively for Graphite and Beryllium. Those are well above the peak values reached in the "accident" case at 450 GeV and will thus lead to even more severe stresses.

Table I. Maximum energy and instantaneous temperature rise for various collimator jaw materials

Material	Density g/cm^3	Max Energy GeV/cm^3	Max Temp ^{o}K	Escaping %
Graphite	1.77	1.3×10^{13}	800	96.4
Beryllium	1.85	0.9×10^{13}	310	97.0
Aluminum	2.70	5.3×10^{13}	2700	88.8
Titanium	4.54	1.7×10^{14}	> 5000	79.5
Copper	8.96	6.4×10^{14}	> 5000	34.4
Graphite + Copper Coating (100μm)	8.96	7.0×10^{14}	> 4000	94.1

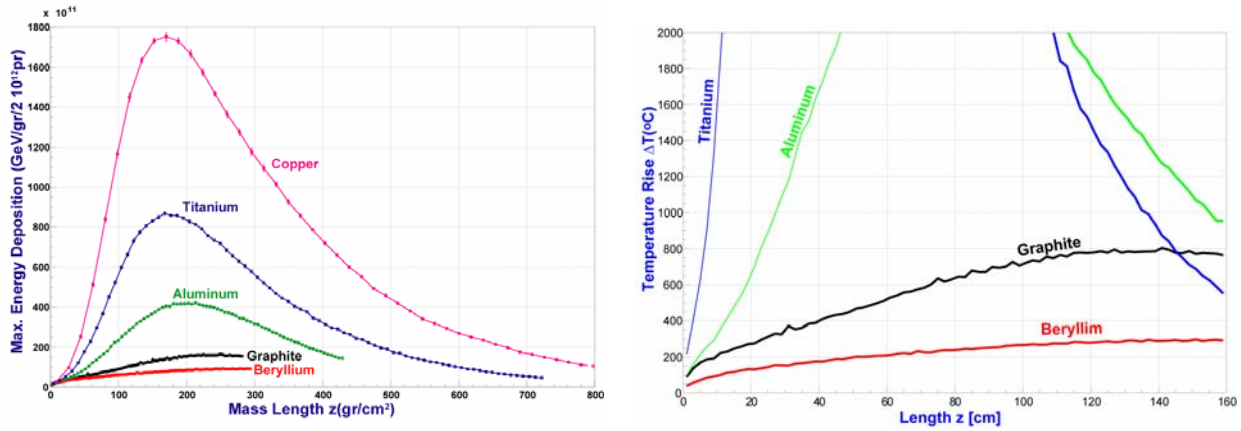

Figure 2. (a) Trace of the maximum energy deposition on a collimator jaw per mass-length, and (b) maximum instantaneous temperature for the wrong kick scenario at 7 TeV/c.

3 PROTECTION OF SUPER-CONDUCTING ELEMENTS

Graphite is chosen as the material for the collimator jaws, since it is the only one to survive the accident case scenario. The simulation effort was concentrated on the effect of the collimators for the various beam loss scenarios along with the normal collimation procedures. In LHC two cleaning insertions are foreseen, the Region 3 (IR3) and Region 7 (IR7) for the momentum and

betatron cleaning, respectively (Fig. **3**a). These regions are dedicated for beam collimation through a two-stage collimation system, the design goals being absorbing part of the primary beam halo and of the secondary radiation. The tertiary halo which escapes the collimation system in IR7 may heat the cold magnets up to unacceptable levels, if no additional absorber is used.

In order to assess the energy deposition in sensitive components, extensive simulations were performed in IR7. The 1.5 km long tunnel section had to be simulated, including the straight section and part of the ARC for both dispersion suppressors on the left and right side (Fig. **3**b). For such a challenging simulation work it was decided to follow a modular approach in the geometry definition with an extensive use of user-written programs, thereby allowing the implementation of all magnets and collimators with high precision, including flanges, steel supports and magnetic fields.

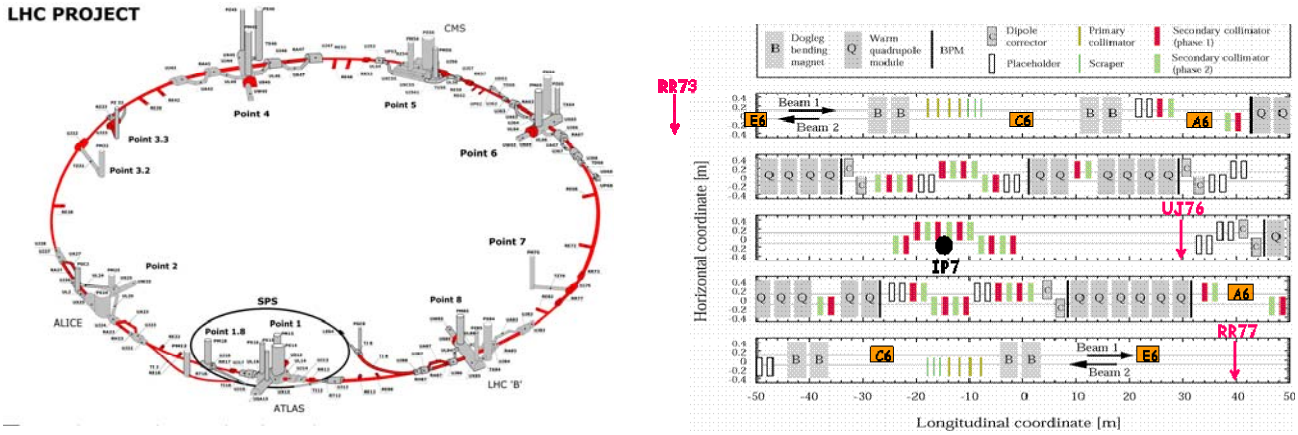

(a) (b)

Figure 3: Schematic view of the CERN LHC accelerator (b) top view of the simulated IR7 geometry.

3.1 Geometry Description

The betatron cleaning insertion mostly consists of conventional magnets, 4 quadrupoles (MQW) to avoid quenches and high heat loads to cryogenics. A pair of warm bending magnets (MBW) increases the beam separation from 19.4 cm to 22.4 cm. A second pair after 340 m downstream (for beam 1) restores to the nominal distance. Each of the warm quadrupoles is composed of 5 MQWA and one MQWB modules (Fig. **4**a), with the same mechanical design. Horizontal and vertical correctors consist of one warm dipole (MCBW). In the dispersion suppressor one can find cold quadrupoles of the MQTL type, orbit correctors (MCB), sextuples (MCS), and cold bending magnets (MB) (Fig. **4**b). The MB's are 14.3 m long objects with a magnetic field of the order of 8 Tesla that bends the 7 TeV beam by 5 mrad. The "sagitta" of these long objects is about 3.5 cm; therefore the internal coils must be bended in the FLUKA geometry definition to follow the beam curvature. This was realized by splitting the MB coils into 4 tilted segments. All the above objects, 23 in total, were modeled with full details and stored in a "parking" area next to the tunnel for latter mapping via the LATTICE card of FLUKA. The transformation of each object was performed by allocating a bounding body in the input file for the replicated item in the geometry, and with the automatically generated

`lattic.f` Fortran routine was making the conversion of the lattice coordinates, to the prototype reference system, located in the parking area.

There are two kind of collimators primary (TCP) and secondary (TCS). The primary collimator (TCP) have 20 cm long graphite jaws with 10 cm of tapering from both sides. The secondaries (TCS) have 100 cm long graphite jaws, plus the 10 cm of tapering on both sides. The collimators were described with all possible details, including the springs, RF-Fingers, collars, cooling pipes, etc. The collimators jaws are sitting at 6 σ for the primaries and 7 σ for the secondaries from the beam orbit. The value of σ depends on the beta function of the beam. Moreover, the tilt of the jaws follows the beam divergence at the location of the collimator. Several ideas have been studied to address the problem of the variable jaws of the collimators, position and tilt. It was decided, to change at runtime the position and orientation of the collimator jaws planes. This was performed inside the `lattic.f` routine, for every single step when a particle entered a new collimator lattice. The beam lines including the surrounding tunnel for the dispersion suppressors and all the elements (more than 200 in total) were automatically generated, by the Rexx [7] script, using the latest beam optics V6.5 [8].

Each LHC magnet has it own magnetic field mapping that is defined in various ways, i.e. analytic form, 2D interpolation grid including possible symmetries. Therefore a special file format was created to allow a common and more flexible description of all cases. The format describes a field by use of a 2D linear interpolated form, or using the analytic form of the field (for constant fields and perfect quadrupoles) or both, includes symmetries and coordinate transformation. For example the field of the quadrupoles, was described inside the vacuum pipes using the analytic form, while outside it was linearly interpolated from a 2D grid. The intensity or the gradient of each magnetic field as well the rotation and positioning in the ARC were dynamically assigned by the generating Rexx script for each element to ensure the correct optics and beta functions of the beam.

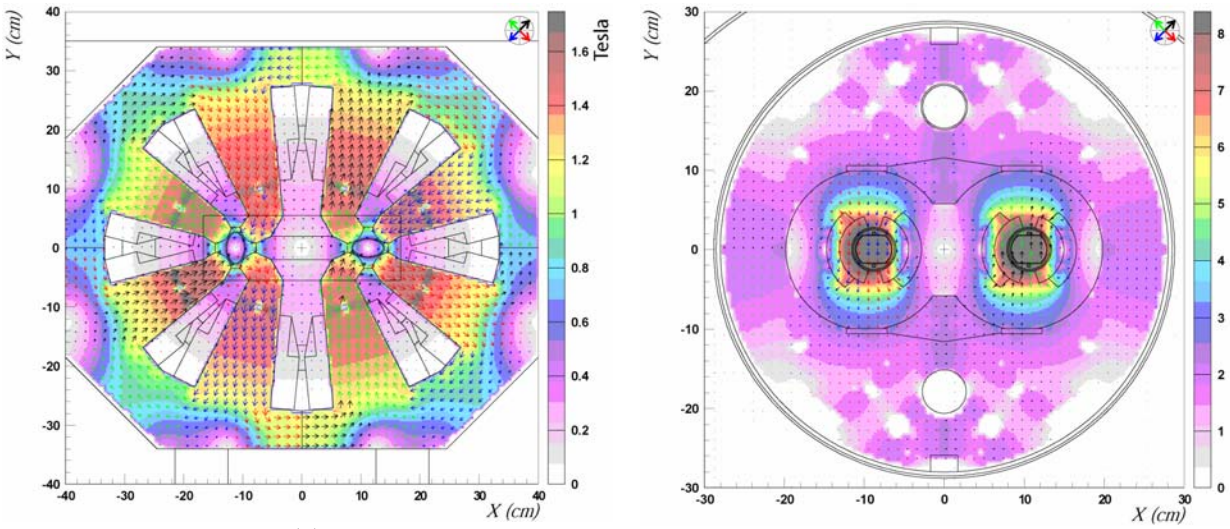

(a) (b)

Figure 4: Cross section of geometry and magnetic field map of (a) warm quadrupole (MQW) and (b) superconducting bending magnet (MB)

For such a cumbersome setup, there is no unique biasing scheme. The applied technique was to adjust the importance of the regions, and to enable Russian roulette splitting of secondaries produced in a collision, inverse proportional to their average distance from each of the two beam lines. However for every simulation run, a dedicated biasing scheme was additionally introduced for the regions of interest.

3.2 Primary inelastic collisions map

The map of the primary inelastic collisions, i.e. the position were the particles are lost on the collimators, was calculated using a multi-turn cleaning process simulated by the COLLTRACK V5.4 [9] code. The program tracked for 100 turns the 7 TeV beam using low beta settings and pencil beam on primary collimator(s) with 0.0025 σ impact parameter, 200 μm spread in the non-collimation plane. When an inelastic interaction takes place, the position and direction of the lost proton is recorded into a file. The individual cascade starts by forcing the FLUKA code to create an inelastic nuclear interaction of a proton inside the collimators jaws at the position given by the tracking program reading randomly the coordinate and the direction of the lost protons.

It is expected that the beam life time during a fill of the LHC may occasionally drop substantially below well below the normal value. The collimation system should therefore be able to handle increased particle losses, in order to avoid beam aborts. In particular, the range of acceptable lifetimes must permit the commissioning of the machine and performance tuning in nominal running. For periods of up to 10 s beam lifetimes of 0.2 h at top energy must also be accepted. For continuous losses a minimum possible lifetime of 1 h is specified for both injection and top energy [10]. They correspond to a peak value of 4×10^{11} p/s collimated per beam, equal to 450 kW of power vanished in the cleaning insertions. The results were either scaled to the peak value of 4×10^{11} p/s lost for the 0.2h beam life time scenario, or to the yearly average which is estimated to be 4.1×10^{16} p/yr during the operation of the LHC. Since the betatron cleaning (IR7) is far away from the high luminosity interaction points, no other source of particle losses were taken into account.

3.3 Results

3.3.1 Collimator heating

The first of the secondary collimators is located 40 m downstream of the primary collimators, the cross-talk between them is quite important. This is due to the resulting transverse momentum, P_t, gained by protons interacting with the nuclei of the collimator jaws. The P_t is expected to be of the order of $P_t \approx 400–500$ MeV/c with a roughly Gaussian shape, typical of hadron-nucleus collisions at high energies because of the intrinsic hadron production P_t and the nuclear Fermi motion. With a beam momentum of 7 TeV/c it yields an average $\langle P_t/P \rangle \approx 70$ μrad, corresponding to almost 3 mm transverse displacement at 40 m distance. Since the object that sit closer to the beam after the primary collimators are the secondary ones, it is expect that a significant part of the cascade will be developed on the secondaries. Indeed the first secondary collimator TCS.A6L7.B1, will receive in total 22 kW of power for the 10 s peak lost beam scenario (Fig. **5**), with the hot spot peaking at 30 W/cm^3. This instantaneous and asymmetric energy deposition of the cascade induces an uneven load and severe stresses on the collimator body. Another important effect is the increase in the water pressure that one expects from the instantaneous

temperature rise on the cooling circuit. It is estimated that an instantaneous increase of 1 degree in the temperature of the cooling water will lead to a pressure bump of 5 atm.

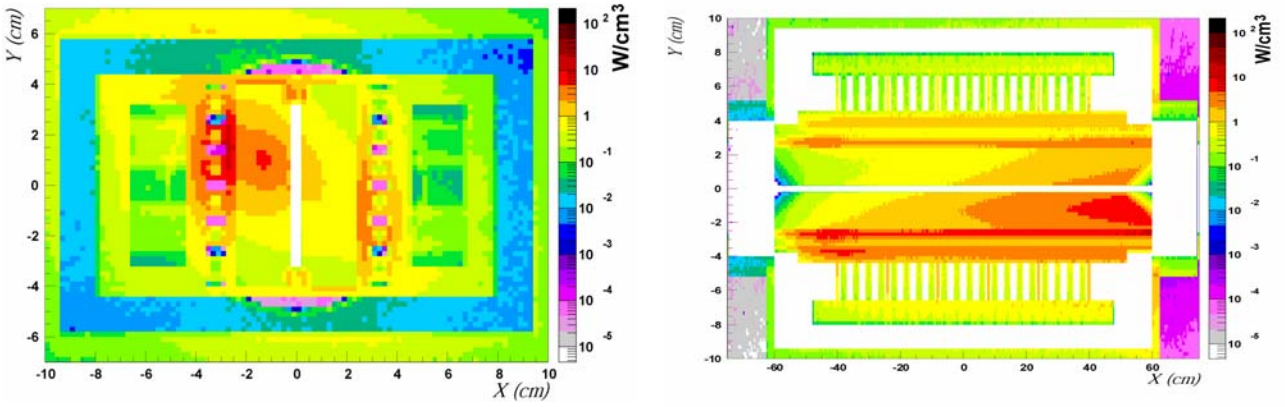

(a) (b)

Figure 5: Energy deposition on the secondary collimator. It is visible the hotspot from the cascade at about 1cm from the center, due to the effect of the magnetic field of the MBW and the rotation of the collimator.

3.3.2 Energy deposition in the superconducting magnets

The radiation level expected in IR7 during operation is very high. Some of the cold magnets will not survive unless adequately protected from radiation. Special equipment (the so-called absorbers) is therefore needed to prevent secondary particles from reaching their superconducting coils. Absorbers were implemented in FLUKA as special secondary collimators with copper jaws and 10 σ half-gap. As for the collimators, absorbers can have any orientation in space. In the present study, only absorbers intersecting the horizontal ("horizontal absorbers") and vertical ("vertical absorbers") component of the halo were considered. Four possible locations were studied (A4, A6, C6, D6), as indicated in figure **1**b. On the one hand, the longer is the distance from the magnet to be shielded the lower is the influence of the absorber on the magnet. On the other hand, if the absorber is too close to the magnet, the cascade generated in the absorber may reach and quench the magnet. A large set of simulations were needed in order to optimize the use of absorbers.

During operation, the largest fraction of particle losses will take place in the first three primary collimators. The distribution of losses will be an average of the following three limit cases: all losses concentrated in the first "vertical scenario", in the second "horizontal scenario" and in the third "skew scenario" collimator. These three scenarios were studied separately.

The initially large number of possible combinations (three scenarios, two absorber orientations, two beams and four locations) was reduced by general considerations after a first set of simulations. Preliminary results already showed that the location A4 is too far away from the cold magnets to be effective. Therefore only locations A6, C6 and E6 were further considered. For almost every absorber orientation and location, the horizontal scenario led to the highest values of energy deposition in the cold coils. Being the most conservative choice, it was taken as the reference case. Moreover, given the symmetry of the setup, only the case of beam 1 was studied.

Despite all these simplifications, a very large number of simulations were needed to obtain good accuracy. The probability of having a particle interacting in a coil 400 m downstream of the collimators is utterly small, because the presence of absorbers reduces the initial radiation levels in the cold aperture by 2 orders of magnitude. Biasing techniques and high energy thresholds in elements in the warm section allowed reducing the CPU time per history from 120 seconds to 2-3 seconds.

The first MQTL is the most sensitive element because of its location relatively close to the collimators. Three absorbers per beam in locations A6 (horizontal absorber), C6 (vertical) and E6 (horizontal) can safely keep the energy deposition in the first MQTL below the quenching limit. Figure **6** shows the reduction of the radiation level in the dispersion suppressor downstream of the last absorber, with respect to the no-absorber case. Configurations with only two absorbers cannot grant sufficient protection. Moreover, introducing a second absorber in location E6 (just in front of the first MQTL), did not prove to be fully efficient. Nevertheless, latest results showed that the energy deposited in the coils of the first two MB's, despite of the three absorbers, is still close to the quenching limit. Further investigation is needed to determine whether a fourth absorber is required and its location.

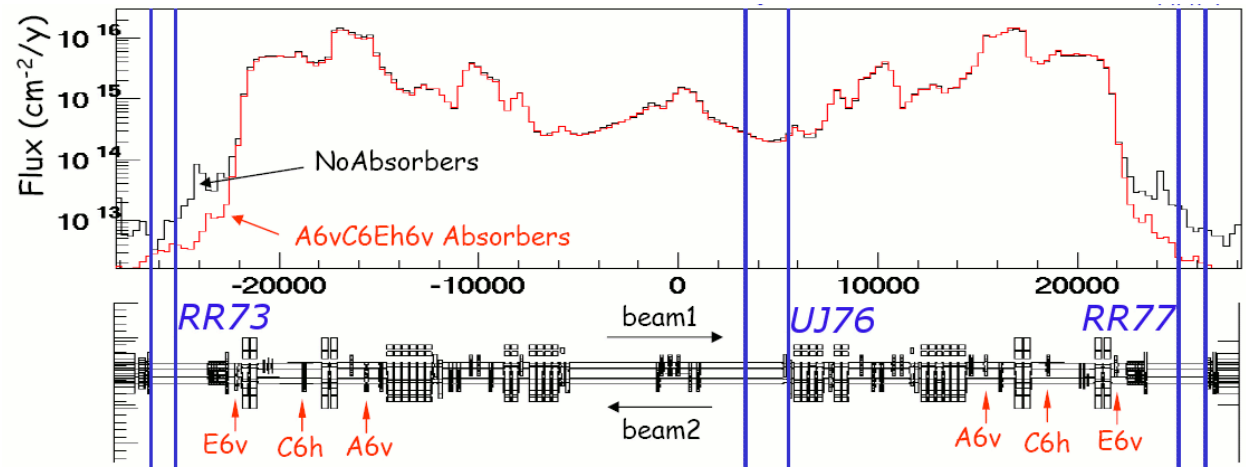

Figure 6: All particle fluence in the IR7 tunnel versus the longitudinal distance. The effect of the additional absorbers is visible in the cold sections.

3.3.3 Perturbation to electronics

The complexity of the LHC accelerator demands the installation of the control electronics close to the beam lines. Control devices for the cryogenics, the vacuum, the quench protection system, the beam diagnostics and instrumentation will have to be installed inside the accelerator tunnel to reduce the cabling costs and the noise-to-signal ratio. Other equipment, like the power converters and the energy extraction system, can be housed in special cavities constructed in transverse positions along the tunnel (Fig. **3**b). All these devices have to operate reliably for a sufficient amount of time (several years, depending on the device) in order to ensure the good functionality of the LHC accelerator.

However, any electronic device operating in strong radiation fields such as those expected for the LHC tunnel will undergo degradation due to radiation damage effects. Energetic particles incident on a semiconductor lose their energy in ionizing and non-ionizing processes as they travel through matter. The ionizing processes involve electron-hole pair production (dark

currents) and the subsequent energy deposition (dose) effects. The non-ionizing processes result mainly in displacement damage effects, i.e. displaced atoms in the detector bulk and hence defects in the semiconductor lattice like vacancies and interstitials. For most of the devices, the displacement damage effects become important for particle fluences above 10^{10} cm^{-2} [11,12].

During the ionization process and under appropriate operating conditions in a device, electrical pulses are generated, which can be large enough to disrupt the normal device operation. The result can be a non-observable effect, a transient disruption of circuit operation, a change of logic state or a permanent damage to the device or integrated circuit. There is not any fluence threshold for this kind of effects since a single particle can create such a failure or a so-called Single Event Effect (SEE). High energy charged hadrons cause SEE through the highly ionizing secondary fragments that they produce when they collide with the silicon nuclei. Neutrons do not create direct ionization, but randomly interact with silicon nuclei generating charged secondary particles, which will further cause ionization and possibly SEE. In general terms, hadrons below 20 MeV seem to be harmless, but SEE might rise rapidly with increasing proton energy. As a result, SEE are expected to be one of the main future concerns related to radiation effects [13,14].

In order to study the radiation tolerance of the LHC electronics, the dose and the hadron fluences were scored at the regions reserved for the electronic equipment. The 1 MeV neutron equivalent fluence for neutrons, protons, pions and electrons is expected to contribute to the determination of the displacement damage [15,16], while the scoring of all hadrons above 20 MeV serves as a good lodestar for the estimation of the SEE expected in the areas of interest. Since the betatron cleaning area will be the hottest region in the LHC tunnel, several shielding scenarios have been applied in order to reduce the radiation levels in the regions of interest.

3.3.4 Simulation accuracy

The systematic error when simulating the cascade of 7 TeV beams is a combination of several factors, in most of the cases very difficult or even impossible to predict. The main sources of errors that can be applied to the previous mentioned simulations, is summarized in the following categories:

- Error due to the physics modeling, *i)* in the uncertainty in the inelastic p-A extrapolation cross section at 7 TeV lab; *ii)* uncertainty in the modeling used from the simulation code. One would expect a factor of 1.3 on the integral quantities scored like energy deposition (peak included), while for multi differential quantities the uncertainty can be much worse.
- Errors due to the assumptions used in the description of the geometry and of the materials under study. Usually it is difficult to quantify this uncertainty; experience has shows that a factor of 2 can be taken as a safe limit [17].
- Errors when having beams grazing at small angles the surfaces of the collimators, where the surface roughness is not taken into account. A factor of 2 can be taken as a safe choice.

4 CONCLUSIONS

The choice of materials for the collimators of the LHC is limited to low Z-materials, like Graphite or Beryllium. This is not due to the normal operational scenarios but rather to accidental, rapid impacts of beams, either at injection or, more severely, during a coast at 7 TeV. For accidents at 7 TeV neither Beryllium nor Graphite will melt locally, but cracks and permanent deformations of the collimator side face have to be expected.

The LHC betatron cleaning insertion has been extensively studied by means of FLUKA simulation, on a 32 CPU Linux cluster. A modular approach in the geometry definition was chosen, and all the relevant elements, magnets and collimators were implemented with high precision. About 10^7 primary particles were totally simulated, with a cumulative time need equal to 9 months. Analysis of the results showed that to prevent superconducting magnets from quench, at least 3 absorbers are needed. The simulation work is still in progress, to investigate the heating on the cold bending magnets (MB), as well the possible addition of shielding on the critical areas to protect the electronic equipments.

5 REFERENCES

1. J.B. Jeanneret, D. Leroy, L. Oberli and T. Trenkler. LHC Project Report 44 (1996).
2. A.Fassó, A.Ferrari, P.R.Sala, "Electron-photon transport in FLUKA: status", *Proceedings of the MonteCarlo 2000 Conference*, Lisbon, October 23-26 2000, A.Kling, F.Barao, M.Nakagawa, L.Tavora, P.Vaz - eds., Springer-Verlag Berlin, p.159-164 (2001).
3. A.Fassó, A.Ferrari, J.Ranft, P.R.Sala, "FLUKA: Status and Prospective for Hadronic Applications", *Proceedings of the MonteCarlo 2000 Conference, Lisbon*, October 23-26 2000, A.Kling, F.Barao, M.Nakagawa, L.Tavora, P.Vaz - eds., Springer-Verlag Berlin, p.955-960 (2001).
4. R. Assmann et al., "Requirements for the LHC Collimation System", *Proceeding of 8th European Particle Accelerator Conference (EPAC02)*, La Vilette, Paris, France 3-7 June 2002 – E.P.S., Geneva, 2002 pp 197. LHC Project Report 599.
5. R. Assmann, B. Goddard, G. Vossenberg, E. Weisse, "The Consequences of Abnormal Beam Dump Actions on the LHC Collimation System", LHC Project Note 293.
6. R. Assmann, C. Fischer, J.B. Jeanneret, R. Schmidt, "Summary of the CERN Meeting on Absorbers and Collimators for the LHC". LHC Project Note 282.
7. V.Vlachoudis, "BRexx Overview", Rexx Symposium 2001, Research Triangle Park, NC May 2001
8. O. Brüning et al, "LHC Design Report. Volume I The LHC Main Ring", 4 June 2004 CERN-2004-003
9. R. Assmann, et al., "Tools for predicting cleaning efficiency in the LHC", CERN-LHC-PROJECT-REPORT-639, Proceedings of Particle Accelerator Conference (PAC 03), Portland, Oregon, 12-16 May 2003
10. R. Assmann, LHC-PROJECT-NOTE-277 (2002)
11. A. H. Johnston, "Displacement Damage and Special Issues for Optoelectronics", March 2002, (http://parts.jpl.nasa.gov/docs/Radcrs_Final6.pdf)

12. G. C. Messenger, " A summary review of Displacement Damage from high energy radiation in silicon semiconductors and semiconductor devices", IEEE Trans. Nucl. Sci. Vol. 39, No. 3, June 1992.
13. H. H. K. Tang, K. P. Rodbell, "Single event upsets in microelectronics: fundamental physics and issues", MRS Bulletin, pp 111-116, February 2003.
14. P. E. Dodd, L. W. Massengill, "Basic mechanisms and modeling of Single-Event Upset in digital microelectronics", IEEE Trans. Nucl. Sci., 50 (3), June 2003.
15. M. Huhtinen and P.A. Aarnio, Pion induced displacement damage in silicon devices, NIM **A** 335, pp. 580-582 1993.
16. G.P. Summers et al., Damage correlations in semiconductors exposed to gamma, electron and proton radiations, IEEE Trans. Nucl. Sci. Vol. 40, No. 6, December 1993
17. M.Huhtinen and N.V.Mokhov, "A Cross-comparison of MARS and FLUKA Simulation Codes", FERMILAB-FN-697 27th Jul 2000